

# Study on contact pressure and wear status of the seal faces under different means to elevate barrier fluid pressure for kettle mechanical seals

LI SHUANGXI, SUN XIANDONG, ZHANG PENG, CAI JINING, WANG LIANG

College of Mechanical and Electrical Engineering

Beijing University of Chemical Technology

No.15, N.3rd Ring Rd chaoyang District, Beijing

CHINA

buctlsx@163.com

*Abstract*—Either barrier fluid pressure constant (BFPC) or barrier fluid differential-pressure constant (BFDPC) is applied for kettle mechanical seals (KMS), large differential-pressure could inevitably appear near the seal faces, resulting in the seal faces deformation and non-uniform contact, aggravating the seal faces wear. In this paper, the maximum seal faces contact pressure under the condition of before wear (BW) and after stable wear (ASW) were calculated by fluid-structure interaction finite element model. Calculating results show that the maximum contact pressure of ASW is lower than that of BW more than 90% for BFPC and BFDPC applied in KMS. In order to study the seal faces wear status under the two kinds of means to elevate barrier fluid pressure, the ratios of the maximum  $p_c V$  values ( $(p_c V)_{\max}$ ) and allowable  $p_c V$  values ( $[p_c V]$ ) of the sealing pair were calculated. Calculating results indicate that the process end seal faces for BFPC applied in KMS, the process end and the atmospheric side seal faces for BFDPC applied in KMS were in alternating wear status, the atmospheric side seal faces for BFPC applied in KMS were in stable wear status. In order to validate the numerical calculation results, verification tests were performed and the friction torques for BFPC applied in KMS were obtained, which were in a good accordance with the calculating results.

Keywords: wear status, contact pressure,  $p_c V$  values, mechanical seal, non-uniform contact

## 1 Introduction

Barrier fluid pressure constant (BFPC) and barrier fluid differential-pressure constant (BFDPC) are two means to elevate barrier fluid pressure for kettle mechanical seals (KMS). For BFPC applied in KMS, barrier fluid pressure is larger than the maximum process pressure constant value, and remains constant during running period of KMS. For BFDPC applied in KMS, barrier fluid pressure is in the step with the process pressure, and is larger than the process pressure constant value. These two means applied in KMS to elevate barrier fluid pressure will inevitably result in the seal faces deformation and aggravating the seal faces wear.

In recent years, many achievements have been attained through the study of contact pressure and wear status on the seal faces. Kleemann and Woydt<sup>[1]</sup> pointed out that the seal faces wear rates decreased with the improvement of surface roughness at a stable friction coefficient. Wen<sup>[2]</sup> found that convergent

nominal clearance caused more serious wear in the inner side than the outer side of the contact area for contact mechanical seal. Zeng<sup>[3]</sup> found that the seal faces wear mark mainly centers on the outer side of the contact area for KMS. Gu<sup>[4]</sup>, Johnson and Schoenheer<sup>[5]</sup> listed wear rates data of the different sealing pair materials in different temperature. Liao<sup>[6]</sup> calculated the seal assembly deformation based on the ring deformation theory. Green<sup>[7]</sup> considered the effect of the fluid film pressure and the contact pressure after wear. Wang<sup>[8]</sup> and S. Shankar<sup>[9]</sup> had conducted research on the seal faces friction characteristics in different media. Peng<sup>[10]</sup> and<sup>[11]</sup> thought that the seal faces wear rate could be aggravated while process parameters changed.

The inevitable seal faces non-uniform contact and wear are important cause for the failure of mechanical seal. To ensure the reliability of mechanical seal and prolong its service life, it is

important to research contact pressure and wear status of the seal faces. The stress field on the seal faces was studied [12-14] and the influence factors of the seal faces friction performance were analyzed [15-17]. In this paper, the maximum seal faces contact pressure and the seal faces wear status had been researched and compared respectively for BFPC and BFDPC applied in KMS, in order to provide theoretical reference for failure of KMS.

## 2 The finite element model of KMS

In this paper, a commonly used structure of KMS was adopted. The sealing pair model was composed of rotating ring, stationary ring and rotating ring seat, as shown in Fig. 1. Since the low rotate speed of KMS, the influence of rotate speed and temperature were ignored, in order to simplify the calculating model. The material properties of the sealing pair are shown in Table 1. The operating parameters of the sealing pair are shown in Table 2.

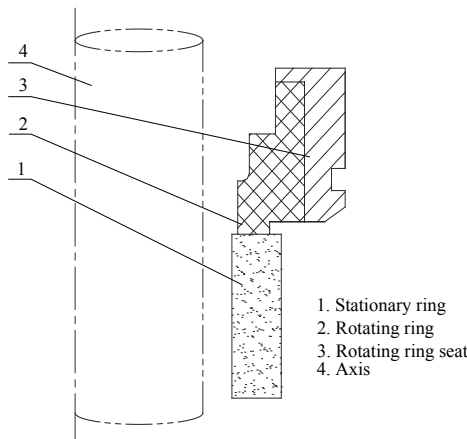


Fig. 1. Structure of the sealing pair

Table 1 Material parameters

| Sealing element    | Material | Elastic modulus | Poisson ratio |
|--------------------|----------|-----------------|---------------|
| Rotating ring      | M106K    | 15 GPa          | 0.27          |
| Stationary ring    | SiC      | 410 GPa         | 0.25          |
| Rotating ring seat | 2205     | 200 GPa         | 0.3           |

Table 2 Operating parameters of the sealing pair

| Barrier fluid | Atmospheric pressure<br>$p_1$ /MPa | Process pressure<br>$p_i$ /MPa | Barrier fluid pressure<br>$p_o$ /MPa |
|---------------|------------------------------------|--------------------------------|--------------------------------------|
| BFPC          | 0                                  | 0.1~2.5                        | 2.7                                  |
| BFDPC         | 0                                  | 0.1~2.5                        | $p_i+0.2$                            |

Since the structure of the sealing pair is rotational symmetry, two-dimensional axisymmetrical model is utilized in finite element analysis (FEA). Plane 42 was adopted in FEA, as it can not only guarantee calculation precision, but also largely improve solving efficiency.

According to the actual structure and size of KMS, the sealing pair finite element model were modeled and contact pairs were used to simulate the contact surfaces interactions, as shown in Fig. 2. Quadrilateral elements were adopted and had been verified by grid independence. There are more than 12000 grids in the finite model.

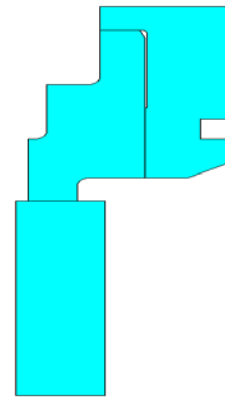


Fig. 2. Finite element model of the sealing pair

There are three kinds of the seal faces wear status while KMS is under the operating conditions: (1) Before wear (BW), the seal faces are parallel planes at free status, as shown in Fig. 2. (2) After pressure has increased, the seal faces are in non-uniform contact status, as shown in Fig. 3. (3) Since non-uniform contact status generates on the seal faces inevitably, the seal faces non-uniform wear will appear after a operating time. In order to make the calculation model more feasible and closer to true situation, initial taper was assumed according to the actual seal faces deformation, as shown in Fig. 4. After stable wear (ASW), the seal faces contact status is shown in Fig. 5.

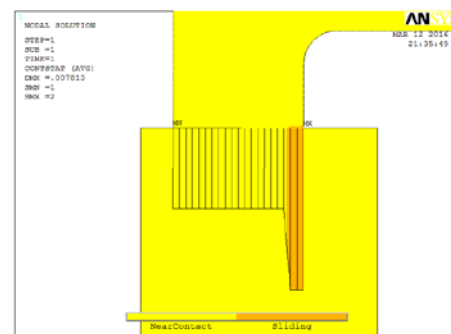


Fig. 3. The seal faces contact status before wear

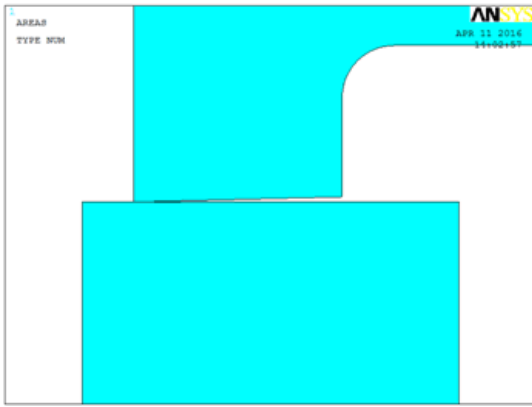


Fig. 4. Certain taper of the seal faces at free state after stable wear

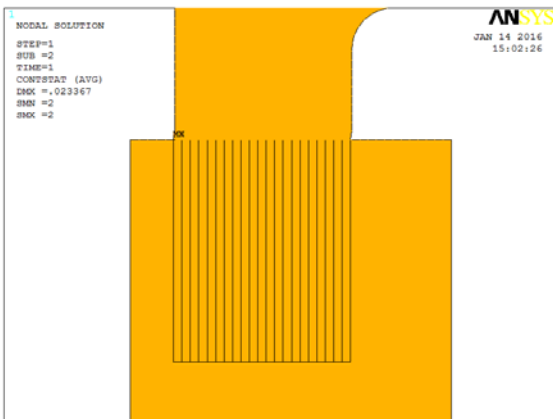


Fig. 5. The seal faces contact status after stable wear

ASW, the seal faces taper angle was solved by the calculation procedure, as shown in Fig. 6. To begin with, initial taper is assumed according to the actual seal faces deformation, then the seal faces contact pressure distribution is attained by FEA results. Next, the ratio  $\delta$  of the difference between the maximum contact pressure ( $p_{max}$ ) and the minimum contact pressure ( $p_{min}$ ) and the sum of  $p_{max}$  and  $p_{min}$  were compared with 5%. If  $\delta < 5\%$ , the error of contact pressure distribution is considered to be acceptable. If  $\delta \geq 5\%$ , the seal faces taper angle will be adjusted and recalculated through the calculation procedure until the seal faces contact pressure distribution is acceptable, then the seal faces taper angle will be outputted.

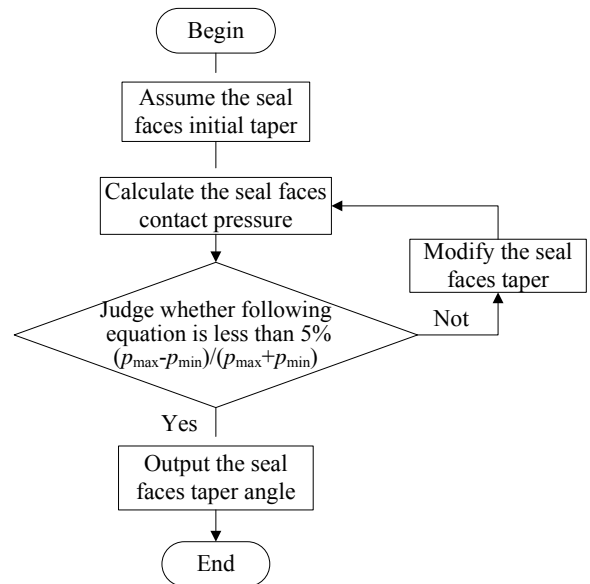


Fig. 6. Calculation procedure of the seal faces taper after stable wear

### 3 Contact pressure and wear status analysis of the seal faces for BFPC applied in KMS

#### 3.1 Contact pressure analysis of the seal faces

For BFPC applied in KMS, the barrier fluid pressure is larger than the maximum process pressure constant value during the running period of KMS. According to the method utilized to solve the taper angle, the process end and the atmospheric side seal faces contact pressure were calculated.

(1) BW and ASW, the maximum process end seal faces contact pressure ( $p_{cmax}$ ) changed with process pressure, as illustrated in Fig. 7.

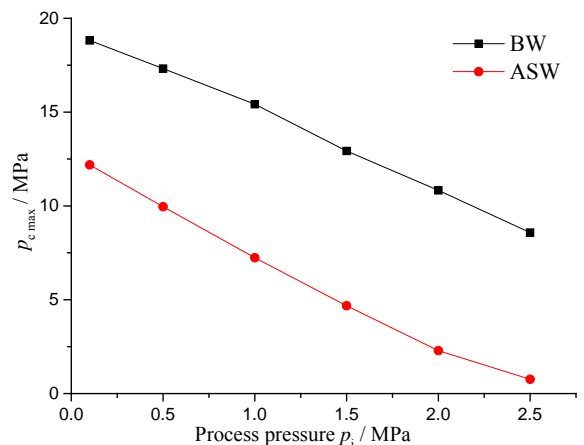


Fig. 7. The maximum process end seal faces contact pressure changed with process pressure

BW, the maximum seal faces contact pressure after process pressure had increased (APPI) decreased 54.42% than that of before process pressure rose

(BPPR). ASW, the maximum seal faces contact pressure APPI decreased 88.19% than that of BPPR. For BFPC applied in KMS, it shows that the maximum seal faces contact pressure decreases with the increment of process pressure.

APPI in kettle, the maximum seal faces contact pressure of ASW decreased 91.14% than that of BW. ASW, the process end seal faces contact status has been improved obviously.

(2) According to the results of BFPC applied in KMS, in atmospheric side, the maximum seal faces contact pressure of BW was 18.82 MPa while the maximum seal faces contact pressure of ASW was 1.18 MPa. The maximum contact pressure of ASW decreased 93.73% than that of BW.

BW, contact pressure mainly focuses on the outside of the seal faces, results in the seal faces being in poor contact status. ASW, the atmospheric side seal faces contact status has also been improved obviously.

### 3.2 Wear status analysis of the seal faces

Only do materials of sealing pair be used in allowable  $p_c V$  values ( $[p_c V]$ ), could they satisfy the requirements of working life and wear rates [4]. According to analytic results of the seal faces contact pressure, the ratios of the maximum  $p_c V$  values  $(p_c V)_{\max}$  and the  $[p_c V]$  were calculated, as illustrated in Fig. 8.

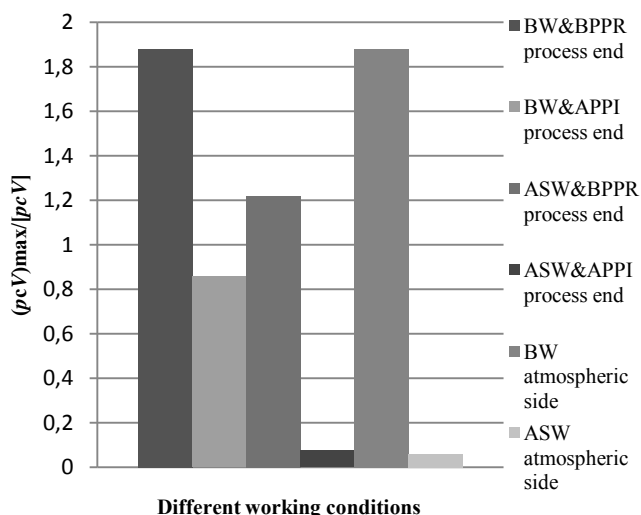


Fig. 8. The ratios of the  $(p_c V)_{\max}$  and the  $[p_c V]$  of the seal faces under the different operating conditions

For process end, it is obvious that the seal faces of ASW&APPI are in good wear status while the seal faces of BW&BPPR are in worse wear status. For atmospheric side, the seal faces of BW are in worse

wear status while the seal faces of ASW are in good wear status.

For BFPC applied in KMS, the process end seal faces are in alternating wear status while the atmospheric side seal faces are in stable wear status under the operating conditions.

## 4 Contact pressure and wear status analysis of the seal faces for BFDPC applied in KMS

### 4.1 Contact pressure analysis of the seal faces

For BFDPC applied in KMS, the barrier fluid pressure is larger than process pressure constant value, and the barrier fluid pressure is in the step with the process pressure. According to the method of solving the taper angle, the process end and the atmospheric side seal faces contact pressure were calculated.

(1) BW and ASW, the maximum process end seal faces contact pressure ( $p_{c\max}$ ) changed with process pressure, as illustrated in Fig. 9.

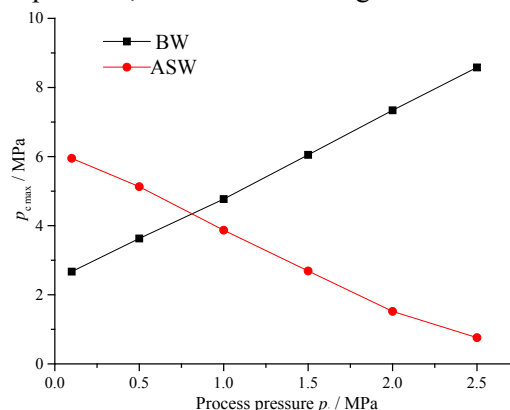


Fig. 9. The maximum process end seal faces contact pressure changed with process pressure

BW, the maximum seal faces contact pressure APPI increased 68.88% than that of BPPR. ASW, the maximum seal faces contact pressure APPI decreased 87.23% than that of BPPR. It shows that the maximum seal faces contact pressure increases with the increment of process pressure BW and decreases with the increment of process pressure ASW.

APPI in kettle, the maximum seal faces contact pressure of ASW decreased 91.14% than that of BW. ASW, the seal faces contact status has been improved obviously.

(2) BW and ASW, the maximum atmospheric side seal faces contact pressure ( $p_{c\max}$ ) changed with process pressure, as illustrated in Fig. 9.

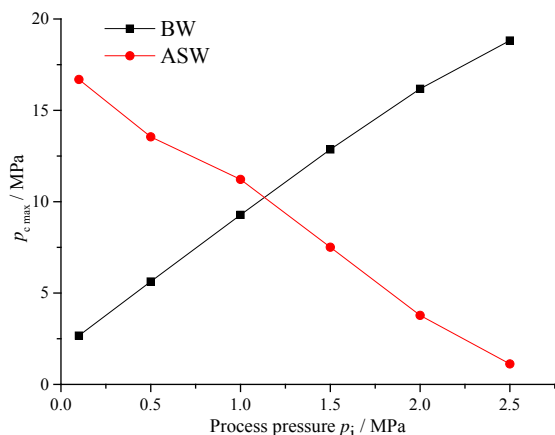


Fig. 10. The maximum atmospheric side seal faces contact pressure changed with process pressure

BW, the maximum seal faces contact pressure APPI increased greatly than that of BPPR. ASW, the maximum seal faces contact pressure APPI had decreased 93.29% than that of BPPR. It shows that the maximum seal faces contact pressure increases with the increment of process pressure BW and decreases with the increment of process pressure ASW.

APPI in kettle, the maximum seal faces contact pressure of ASW had decreased 94.05% than that of BW. ASW, the seal faces contact status has also been improved obviously.

#### 4.2 Wear status analysis of the seal faces

According to analytic results of the seal faces contact pressure for BFDPC applied in KMS, the ratios of the  $(p_c V)_{max}$  and the  $[p_c V]$  were calculated, as illustrated in Fig. 11.

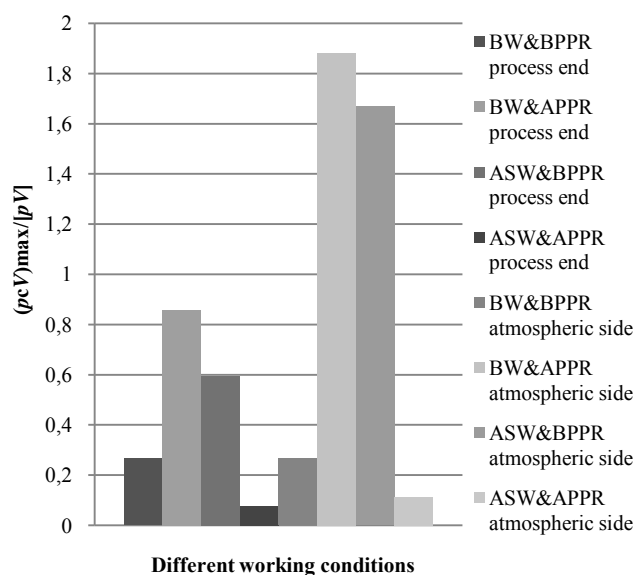


Fig. 11. The ratios of the  $(p_c V)_{max}$  and the  $[p_c V]$  of the seal faces under the different operating conditions

For process end and atmospheric side, the seal faces of BW&APPI are in worse wear status while the seal faces of ASW&APPI are in good wear status.

For BFDPC applied in KBC, the process end and atmospheric side seal faces are in alternating wear status under the operating conditions.

According to Fig. 10 and Fig. 11, the atmospheric side seal faces of BFPC applied in KMS are in best wear status, and the atmospheric side seal faces of BFDPC applied in KMS are in worst wear status. The process end seal faces wear status of BFDPC applied in KMS is better than that of BFPC applied in KMS.

### 5 Verifying contact status

As a result of the specific characteristics of mechanical seal, it is difficult to obtain the seal faces contact pressure under the operating conditions. But it is relatively easier to measure the friction torques between the seal faces and the rotation axis, which is deeply connected to contact pressure and contact status of the seal faces.

Table 3 Friction torques expression

| Calculation basis               | Friction torques |
|---------------------------------|------------------|
| Test values of BW               | $T_{r1}$         |
| Test values of ASW              | $T_{r1}'$        |
| Calculated by integral of BW    | $T_{r2}$         |
| Calculated by integral of ASW   | $T_{r2}'$        |
| Results from empirical formulae | $T_{r3}$         |

In this paper, BFPC applied in KMS was utilized to verify the calculating results. Five kinds of friction torques values were obtained and analyzed, and friction torques expression are shown in Table 3.

$T_{r1}$  and  $T_{r1}'$  were measured from BFPC applied in KMS. The experimental device is showed in Fig. 12.



Fig. 12. The experimental device for measuring friction torques

$T_{r2}$  and  $T_{r2}'$  were calculated by integral, and the seal faces contact pressure values were from FEA results, calculation equation is as follows:

$$T_{r2} = 2\pi r \int p_c \cdot r^2 \cdot r$$

Where  $f$  represents the seal faces friction coefficient, in this paper,  $f=0.08$ .  $r$  represents the radius of the seal faces, mm.  $p_c$  represents the seal faces contact pressure values, calculated by FEA, MPa.

$T_{r3}$  were calculated by average contact pressure, calculation equation is as follows:

$$T_{r3} = p_c \cdot A \cdot f \cdot d_m / 2$$

Where  $A$  represents contact area of the seal faces,  $mm^2$ .  $d_m$  represents average diameter of the seal faces, mm.  $p_c$  represents the average seal faces contact pressure, MPa.

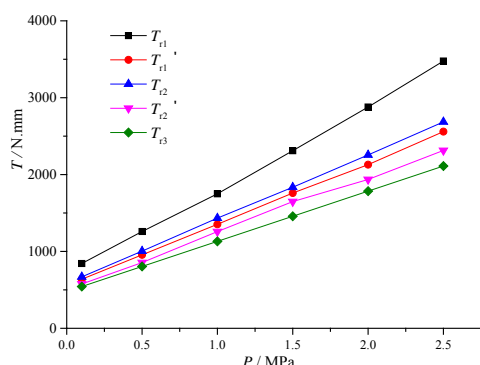


Fig. 13. The friction torques changed with process pressure

The Fig. 13 shows that the friction torques  $T_{r2}$  and  $T_{r2}'$ , calculated from finite element method, are closer to the measured value  $T_{r1}$  and  $T_{r1}'$ . It is

obvious that there is a significant difference between  $T_{r1}$  and  $T_{r3}$ . These datum verify the accuracy of the former calculating results.

The main reason is that  $p_c$  of  $T_{r3}$  were regarded as uniform distribution without considering the influences of the seal faces deformation. Before wear, contact pressure mainly focuses on the outside of the seal faces, which enlarges the friction torques observably. After stable wear, the actual seal faces contact pressure and the calculating seal faces contact pressure tend to distribute uniformly, which results in the empirical formulae values being close to the calculating values by FEA and test values.

## 6 Conclusions

In this paper, the seal faces wear status of BFPC and BFDPC applied in KMS were analyzed under the different operating conditions. The main conclusions are as follows:

(1) For BFPC and BFDPC applied in KMS, the maximum seal faces contact pressure of ASW decreases more than 90% than that of BW.

(2) For BFPC applied in KBC, the process end seal faces are in alternating wear status while the atmospheric side seal faces are in stable wear status under the operating conditions. For BFDPC applied in KBC, the process end and the atmospheric side seal faces are in alternating wear status under the operating conditions.

(3) Based on analysis of the seal faces wear status, the atmospheric side seal faces of BFPC applied in KMS are in best wear status, the process end seal faces of BFDPC applied in KMS take the second place, the process end seal faces of BFPC applied in KMS take the third place, and the atmospheric side seal faces of BFDPC applied in KMS are in worst wear status.

(4) The friction torques experiment verified that the seal faces deformation will result in the seal faces contact pressure distribution non-uniform. The calculating results of the seal faces contact pressure and wear status by FEA are credible. It also indicates that the friction torques values calculated from empirical formulae is basically usable for ASW under the operating condition.



*References*

- 1 Jens Kleemann, Mathias Woydt. Dry friction and wear rates as under liquid lubrication of ceramic/carbon couples up to 450 °C . Industrial Lubrication and Tribology, 2004, 56( 1) : 38-51.
- 2 Wen Qingfeng, LIU Ying, Huang Weifeng, Suo Shuangfu, Wang Yuming. The effect of surface roughness on thermal-elasto- hydrodynamic model of contact mechanical seals. Science China (Physics, Mechanics& Astronomy), 2013, 10: 1920-1929.
- 3 Zeng Hongsheng. Discuss kettle mechanical seal from the chlorination reaction kettle mechanical seal troubleshooting examples. Public Communication of Science & Technology, 2011, 02:75-76+65.
- 4 Gu Yongquan. Mechanical face seal. Dong ying: Petroleum University Publishing House, 1994
- 5 Johnson R L, Schoenheer K. Seal Wear. Wear Control Handbook. 1980: 727-752.
- 6 Liao Chuanjun, Huang Weifeng , Suo Shuangfu, Liu Xiangfeng & Wang Yuming. Fluid-solid strong-interaction model of mechanical seals in reactor coolant pumps. Science China (Technological Sciences), 2011, 9:2339-2348
- 7 Green I. A transient dynamic analysis of mechanical seals including asperity contact and face deformation. Tribology Transaction, 2002, 45( 3) : 284-293.
- 8 Wang J L, Jia Q, Yuan X Y, Wang S P. Experimental study on friction and wear behaviour of amorphous carbon coatings for mechanical seals in cryogenic environment. Applied Surface Science, 2012, 258:9531-9535
- 9 S. Shankar , G. Praveenkumar, P. Krishna kumar. Experimental study on frictional characteristics of tungsten carbide versus carbon as mechanical seals under dry and eco-friendly lubrications. Refractory Metals and Hard Materials, 2016, 54:39-45
- 10 Peng Xudong, Jiao Yurui, Ye Zhiwei, Peng Lianjun. Hot Issues of Mechanical face seal technology. General Machinery, 2003, 03:54-57.
- 11 Peng Xudong, Xie Youbo, Gu Yongquan. The determination of the temperature on seal faces of Mechanical seal. Chemical Engineering & Machinery, 1996, 06:25-28+21+58.
- 12 Wu Wen. Mechanical seal face stress numerical analysis. Xi'an Shiyou University, 2011.
- 13 Zhu Xueming. Research on numerical analysis and optimization of mechanical sealing performance. Wuhan: Wuhan University of Technology, 2005.
- 14 Li Shuangxi, Huang Kesong, Cai Jining, Zhang Qiuxiang, Fu Tonghui. Study on contact state and pressure of process pressure mechanical seals. Lubrication Engineering, 2016,01:10-14
- 15 Zeng Tao. Analysis of influence factors of friction performance on mechanical seals. Lubrication Engineering, 2000, 03:60-61.
- 16 Sun Jiapeng, Yang Qingxiang, Song Baoyu. Analysis of affecting factor of mechanical seal material match friction coefficient. Mechanical Transmission, 2012, 12:98-101.
- 17 Wei Long, Zhang Penggao, Liu Qihe, Jin Liang, Fang Guifang. Influencing factors analysis and experiments of friction coefficient between the end faces for contact mechanical seals. Tribology, 2016, 03:354-361.